Remote Sens. **2011**, *3*, 1691-1709; doi:10.3390/rs3081691

OPEN ACCESS

Remote Sensing

ISSN 2072-4292

www.mdpi.com/journal/remotesensing

Article

Deriving Fuel Mass by Size Class in Douglas-fir (*Pseudotsuga menziesii*) Using Terrestrial Laser Scanning

Carl Seielstad *, Crystal Stonesifer , Eric Rowell and Lloyd Queen

National Center for Landscape Fire Analysis, College of Forestry and Conservation, The University of Montana, Missoula, MT 59812, USA; E-Mails: csstonesifer@fs.fed.us (C.S.); eric.rowell@firecenter.umt.edu (E.R.); lloyd.queen@firecenter.umt.edu(L.Q.)

* Author to whom correspondence should be addressed; E-Mail: carl.seielstad@firecenter.umt.edu; Tel.: +1-406-243-6200; Fax: +1-406-243-2000.

Received: 1 July 2011; in revised form: 26 July 2011 / Accepted: 4 August 2011 / Published: 16 August 2011

Abstract: Requirements for describing coniferous forests are changing in response to wildfire concerns, bio-energy needs, and climate change interests. At the same time, technology advancements are transforming how forest properties can be measured. Terrestrial Laser Scanning (TLS) is yielding promising results for measuring tree biomass parameters that, historically, have required costly destructive sampling and resulted in small sample sizes. Here we investigate whether TLS intensity data can be used to distinguish foliage and small branches (≤0.635 cm diameter; coincident with the one-hour timelag fuel size class) from larger branchwood (>0.635 cm) in Douglas-fir (*Pseudotsuga menziesii*) branch specimens. We also consider the use of laser density for predicting biomass by size class. Measurements are addressed across multiple ranges and scan angles. Results show TLS capable of distinguishing fine fuels from branches at a threshold of one standard deviation above mean intensity. Additionally, the relationship between return density and biomass is linear by fuel type for fine fuels (r^2 = 0.898; SE 22.7%) and branchwood (r^2 = 0.937; SE 28.9%), as well as for total mass (r^2 = 0.940; SE 25.5%). Intensity decays predictably as scan distances increase; however, the range-intensity relationship is best described by an exponential model rather than $1/d^2$. Scan angle appears to have no systematic effect on fine fuel discrimination, while some differences are observed in density-mass relationships with changing angles due to shadowing.

Keywords: Terrestrial Laser Scanning (TLS); Douglas-fir (*Pseudotsuga menziesii*); biomass; canopy fine fuels; intensity

1. Introduction

The application of Terrestrial Laser Scanning (TLS) in biological systems such as forests has grown rapidly. The focus has been on determination of stand characteristics such as tree locations, heights, and diameters (e.g., [1,2]), more recently evolving to measurements of canopy structural metrics like canopy gap fraction and leaf area (e.g., [3]). TLS is currently being used to produce representative crown density profiles for several conifer species in the western US [4] to support development of robust biomass equations based on large sample sizes. This research exploits randomized branch sampling [5] coincident with laser scans of trees and is predicated on understanding the fundamental characteristics of laser intensity and density data from foliage and branches.

The utility of TLS reflectance intensity data is largely unknown. In one of the few published studies, Franceschi *et al.* [6] used TLS intensity to discriminate effectively between H_2O-bearing minerals in lithologic sections of limestone and marl. In related laboratory work, Pesci and Teza [7] showed that surfaces having irregularities smaller than the footprint of the laser are Lambertian, while flat surfaces produce brighter reflections that vary as a function of viewing angle. These results suggest that needles and small branches of conifer trees might produce dim reflections of near-constant intensity relative to larger branches and boles. In practice, this is what we have observed in scanned images of conifer specimens.

In this study, we examine the ability of a near-infrared TLS instrument to discriminate fine fuels from branchwood in Douglas-fir (*Pseudotsuga menziesii*) branch specimens. Kaasalainen *et al.* [8] showed that the effects of distance and target reflectance on recorded intensity are highly variable in TLS systems; hence, we address measurements across ranges and scan angles. We systematically image Douglas-fir branch specimens from multiple distances and perspectives, separate the fine fuels ($\leq$0.635 cm diameter) from each branch, then dry and weigh the samples by size class and compare with laser intensity and density data. In our study, fine fuel is classified in accordance with American timelag fuel conventions [9] differing somewhat from others [10] who have used a threshold of 0.33 cm for estimating canopy bulk density for crown fire modeling. Accordingly, we classify branchwood as anything larger than 0.635 cm diameter.

By comparing biomass measurements with laser-derived reflection intensity and return density, we propose to determine whether a TLS system can produce results similar to those obtained from destructive sampling. However, the effects of shadowing of interior elements by tree or branch hulls are unknown, while range and angle dependencies caused by variable target geometry are likely to influence the partitioning of crown fuels by size class. Hosoi and Omasa [11] and Loudermilk *et al.* [12] have over-sampled objects from multiple viewing angles to address the former issue, but this labor-intensive approach defeats a larger purpose of someday using TLS to obtain large samples of trees quickly and easily. Therefore, we investigate range and angle effects on fuel size class discrimination and biomass estimation from single scans of tree branches, with the long-term goal of increasing the efficiency of biomass sampling using TLS. Additionally, we attempt to improve understanding of the TLS instrument used here for a growing forestry user community.

Objectives of this study are as follows:

1. Describe instrument range dependencies using a calibrated target and Douglas-fir branches.
2. Discriminate fine fuels from branchwood using laser intensity data.

3. Quantify relationships between laser density and mass for fine fuels and branchwood.
4. Identify effects of scan angle on fine fuels discrimination and biomass estimation.

2. Methods

2.1. The Instrument

Time-of-flight terrestrial laser scanners compute ranges to objects, similar to laser rangefinders. TLS systems scan on user-specified angular grids to produce point clouds with accurate spatial coordinates and reflection intensities for the objects of interest. In this study, an Optech ILRIS®3_6HD-ER was used to image branches of Douglas-fir at multiple ranges and angles.

The instrument uses a class I laser (1,535 nm wavelength) to provide ranges to objects located 3 to 1,500 m from the viewing station. Beam divergence is 150 μrad resulting in a laser spot size of 29 mm at a 100 m range ($0.17R + dl$, where R = range in meters and dl = diffraction limit of 12 mm), with published range and angular accuracies at the same distance of 7 mm and 8 mm, respectively. Technological advances are constantly improving the speed and range of TLS. Our instrument scans at 10 kHz to 800 m on a 20% reflectivity target, producing five million points in approximately eight minutes. The battery-powered instrument is relatively portable, mounts on a tripod, and scans a full hemisphere. It is controlled by a handheld computer or laptop.

TLS systems have traditionally been used for survey applications, thus intensity data from TLS typically provide image contrast and have not been widely used analytically due to uncertainties about consistency and accuracy. The airborne laser altimetry community has faced similar issues for the past decade [13]. The Optech ILRIS 3_6HD-ER records intensity using two gain settings, which complicates analysis of the data. Bright reflections (≥200 Digital Number (DN)) are recorded in 8 bits, and dim reflections (<200 DN) are recorded separately, also in 8 bits. In a conventional dataset, the ILRIS parser produces a scaled intensity dataset in which high gain values are distributed between 0 and 255 and low gain values are distributed between 300 and 25,500. The high gain values are recorded in single integer DN increments, while the low gain values are binned in 100 DN increments (Table 1). The result is an inconsistently scaled image with artificially high contrast and limited analytical utility. Although the data range implies 16 bit radiometric resolution, partitioning of the data into 512 bins (e.g., 256 bins, twice) effectively results in 9 bit data.

Table 1. Optech ILRIS 3_6HD-ER raw data parameters.

Channel	Minimum Value	Maximum Value	Interval	Range
High gain	0	255	1 DN	0, 1, 2, …, 255
Low gain	300	25,500	100 DNs	300, 400, 500, …, 25,500

In this study, we avoided the data scaling issue by examining high gain and low gain data independently. This is made possible by an integer flag in the raw parser output that denotes which gain setting each shot used. As discussed in more detail below, a comparison of data from each gain setting showed that, within ranges of 15–45 m, the low gain data contained nearly all of the intensity information content; thus, the experiment was simplified by using only the low gain data for analysis.

2.2. The Experiment

Ten Douglas-fir branches were cut from ten trees within a single stand at Lubrecht Experimental Forest, MT, USA. The branches ranged in mass from 100 to 2,200 g (dry weight) and contained material up to 5.5 cm in diameter. Douglas-fir needles are short (up to 2.5 cm) and flat with blunt tips, and completely encircle smooth, flexible branches. The branch specimens were obtained from second-growth (~80 years old) trees in a moderately open, mesic site, mixed with ponderosa pine (*Pinus ponderosa*), typical of lower elevations in the Northern Rocky Mountains. The branches were selected from similar crown positions and orientations and were scanned and destructively sampled within two days of harvest. To test the effects of range and angle on intensity values, each branch was scanned at four ranges (15 m, 25 m, 35 m, and 45 m) and at randomly assigned branch angles. Corresponding spot sizes associated with these ranges are 14.6 mm, 16.3 mm, 18.0 mm, and 19.7 mm, respectively. For each range, an angular step was chosen in order to maintain 4 mm spot spacing. Each branch was mounted on a tripod and positioned so that orientation was as it would be on the tree, with the branch angle perpendicular to the scan angle (0° position; Figure 1). Additionally, each branch was scanned in the 0° position at 15 m, 25 m, 35 m, and 45 m. Range was varied by moving the tripod holding the specimen to pre-measured monuments while holding the scanner viewing station constant. Branches were then pre-assigned randomly angled scans so that each of four additional angles (45°, 90°, 45° up, 45° down) were represented at least four times (Figure 2). All branch angle variations were scanned at constant range (25 m). In sum, range effects were evaluated between 15 and 45 m with branch orientation held constant, and angle effects were evaluated at 25 m with range held constant.

Each branch was then pruned to remove all material with a diameter less than or equal to 0.635 cm (representing the one-hour timelag fuel class threshold) and scanned again at the 25 m, 0° position. Branch material was bagged, labeled, oven dried at 100 °C for four days, and weighed by fuel size class per branch. To assess range effects on a target of known reflectivity, a calibrated 98.7% albedo Spectralon tile was also scanned at 5 m increments from 15 to 100 m at 4 mm spot spacing.

Figure 1. Douglas-fir specimen mounted on tripod in the 0° position.

Figure 2. Sample branch scan angles include 0°, 45°, 90°, 45° up, and 45° down. The **(a)** 0°, **(b)** 45°, and **(c)** 90° positions all maintain the branch in the neutral horizontal position as it would be on the bole of the tree, with the branch angle rotated around the vertical (*z*) axis. In contrast, the **(d)** 45° and **(e)** 90° positions depict the underside and top views of the branch (rotated around the horizontal, or *x*-axis) as the branch faces the scanner head on, simulating the effects of a scan from above or below the crown.

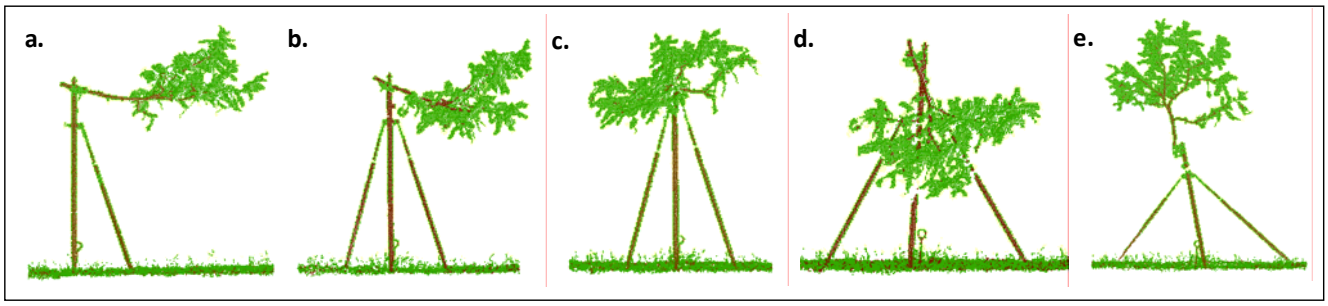

2.3. Data Processing

Raw scan data were converted to text files with Cartesian *x*, *y*, *z* coordinates and 8-bit intensity corresponding to the respective high gain or low gain data scales. Intensity was corrected for range using empirically-derived exponential functions for each gain scale and normalized to the 15 m range. The behavior of intensity data inside 15 m is uncertain [6], hence our use of this minimum range threshold. Range normalization equations were obtained by fitting many decay functions to branch and Spectralon mean intensity data and selecting the best fits as characterized by the coefficient of determination (r^2) and standard error. Coefficients for exponentials were found by using a linear least squares fitting of logarithmic quantities. Each file was edited to remove returns from the tripod, foreground, and background, and a feature attribute table was produced for statistical analysis.

In order to compare intensity distributions of fuels by size class, samples of laser returns representing canopy fine fuels and branchwood were randomly selected from each scan in the following way. First, branchwood returns were removed manually by cross-referencing the digital image with coincident high-resolution photographs of both the native branch and the same branch with its fine fuels removed. Although branchwood is clearly distinct in the images, we acknowledge the chance that some branchwood is erroneously included in fine fuel samples. Next, a random sample of canopy fine fuel returns was generated with a Python script employing the Random Module, which uses the Mersenne Twister as the core random number generator [14]. Three samples with n = 1,000 returns each were produced for 10 branches, across four ranges and five angles. The same process was repeated for the 10 defoliated branch scans; however, due to the smaller pool of returns, sample size was reduced to 500 returns each. Since the fine fuels were physically removed from the defoliated branch before it was scanned, all returns were definitively from the fuel class of interest (branchwood). Defoliated branches were scanned at a range of 25 m and in the 0° position. Due to the small size of some branches, not all branches contributed three separate samples to the pool; thus, 21 total wood samples were generated.

2.4. Analysis

Nonlinear regression was used to assess the effects of range on raw intensity data. Once a suitable range correction equation was derived and applied, box-and-whisker plots were generated to compare the range-corrected result by target material (*i.e.*, foliage, branch, Spectralon). Range-corrected intensity data from canopy fine fuels and branchwood were also assessed using box-and-whisker plots and histograms to evaluate the distinctiveness of their probability density functions. Fine fuels were distinguished from branchwood through trial and error by identifying a threshold intensity separating dim returns (fine fuels) from bright returns (branchwood). Lastly, linear regression was used to document relationships between return density and branch mass by size class, and to assess scan angle effects on mass prediction.

The threshold intensity used to distinguish fine fuels from branchwood was corroborated using two other classification schemes available in common spatial software packages; Fisher-Jenks Natural Breaks (ESRI® ArcMap™ 10.0) and ISODATA (ERDAS IMAGINE® 2010). In short, both methods begin with arbitrary sets of classes. Data values are added to classes based on proximity to class means, and deviations are subsequently calculated around class means. Data values are then moved iteratively between classes in an attempt to reduce total variance. The result is an objective classification of data values, constrained by different user inputs for the two techniques. In the Fisher-Jenks case, the user specifies a number of classes and the algorithm develops an optimal solution for that number. In ISODATA, the user specifies a maximum number of classes and iterations, and the algorithm moves data values and splits/merges clusters until change between iteration is small. In this analysis, the natural breaks classification was run for two classes and ISODATA was run for a maximum of ten classes and ten iterations. As noted above, the classification techniques used in this analysis were employed solely to confirm the quality of the threshold intensity determined through trial and error.

2.5. Practical Considerations of Data Collection and Processing

Each branch scan took approximately 60 seconds of instrument time, not considering set-up of instrument and tripod. Collectively, the fifty-two scans took about 12 hours, highlighting the time needed to prepare individual branches for scanning. Analysis was completed on a personal workstation (Intel Xeon 5160 CPU at 3.00 GHz; 3.00 GB of RAM). Data were parsed and exported as *xyzi* using manufacturer software, then imported into ESRI ArcMap10.0 for spatial editing. Editing was time consuming because the tripod, foreground, and background were removed by hand. Other analyses such as range correction and classification were completed using simple Python scripts and batch processing functionality built into ArcMap, which was made possible because the conversions, imports, and, calculations were the same for each file. We estimate about 1.5 hours per scan for a total ~80 hours to prepare data for analysis. With an established workflow, processing time could be reduced by more than one half, and we note that the individual process is quite fast. However, organizing, editing, and converting data is time consuming. It is also worth considering that expectations for processing efficiency based on this study probably do not apply to larger scans, particularly those requiring multiple scan angles. For example, we were unable to complete the

described processing methods on scans of whole trees (~30 m in height) due to memory limitations of the workstation. Further, stitching multiple scans together is made possible using specific software such as Innovmetric Polyworks® and Leica Cyclone®, which invariably compromise the integrity of intensity data, thereby requiring multiple conversion scripts on both ends of the processing stream.

2.6. Instrument Sensitivity

Examination of many data sets under a variety of acquisition parameters revealed some unexpected behaviors of the Optech ILRIS 3_6HD-ER. First, the instrument is very sensitive, as indicated by the almost complete opacity of individual branches (Figure 3). This suggests that for objects like trees, much biomass is obscured by fine fuels and branchwood located in the object's hull. Several authors [11,12,15] have shown that by scanning from up to seven different viewing stations, this issue can be largely overcome. Second, objects imaged directly in front of, and in close proximity to highly reflective hard targets such as walls exhibit a ghosting effect, in which the locations of some returns along edges are erroneously displaced away from the instrument (Figure 4). This appears to be a ranging issue associated with the algorithm that converts a continuous signal into a discrete distance, and although it is not discernable in scans of complex objects such as trees, it may be present and affect the accuracy of biomass partitioning in three dimensions. Third, instrument sensitivity combined with the use of dual gain settings leads to haloing (described in Section 3.1, directly below) of scanned objects at scan distances of 15 to 45 m (Figure 5). Our results suggest that inside of 45 m, high gain returns can be ignored in assessments of Douglas-fir biomass. However, the presence of a halo of high gain returns might ultimately prove useful in derivations of object volume.

Figure 3. Scan of a Douglas-fir branch on a tripod positioned several meters in front of a wall demonstrating branch opacity. The red points indicate returns from the tripod and branch, and the grey points are returns from the wall.

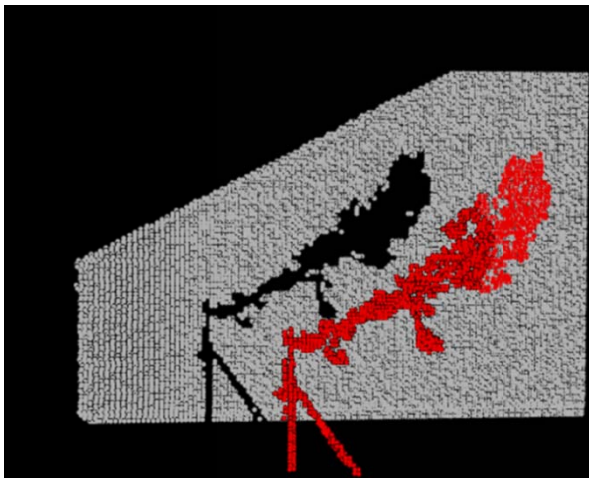

Figure 4. Ghosting phenomenon. Here a tripod-mounted Douglas-fir branch (red) is positioned less than 1 m in front of a classroom whiteboard (white). The trailing returns from the edges of the branch do not represent real reflective surfaces in the scan.

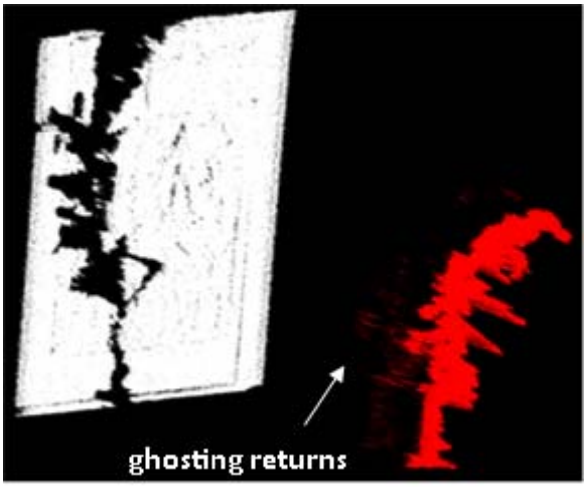

Figure 5. Scanned Douglas-fir branch on a tripod at 25 m showing the distribution of high gain (black areas) and low gain data (green areas). Dim returns recorded by the high gain receiver occur when the laser encounters a very small amount of material in the laser footprint, e.g., flying insects, airborne particulate matter, tips of grass stalks, or the edges of the branch or tripod.

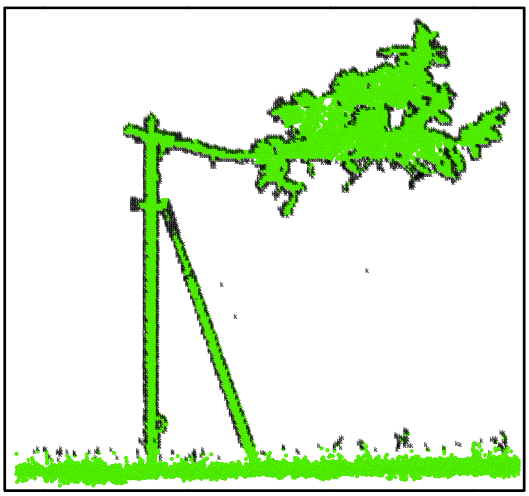

3. Results and Discussion

3.1. High Gain vs. *Low Gain Data*

As noted previously, a high gain receiver on the Optech ILRIS 3_6HD-ER registers intensity data from dim reflections, and a low gain receiver records bright reflections. For close-range scans (e.g., 15–40 m), high gain returns manifest as an annulus of reflections surrounding the scanned object, where the footprint of the laser is fractionally occupied by matter. This halo occurs on all scanned objects with edges and is wider when edges are diffuse or rounded. Predictably, as the distance from the scanner

increases, the proportion of total returns registered by the high gain receiver increases (Table 2), a function of both target reflection efficiency and laser spot size.

Table 2. Proportion of total returns for Douglas-fir branch scans recorded by the high gain and low gain receivers across a series of ranges (and spot sizes).

Distance from Scanner (m)	High Gain (%)	Low Gain (%)	Spot Size (mm)
15	15.1	84.9	14.6
25	20.3	79.7	16.3
35	29.5	70.5	18.0
45	45.4	54.6	19.7

At shorter ranges (<45 m) halo returns are registered by the high gain receiver on the instrument. As the target is moved farther from the scanner, more returns are registered as high gain, until a point is reached when all data are high gain. This distance is target reflectance-dependent. With close-range scans of Douglas-fir branches, the majority of intensity information is derived from low gain data (~80%), and the high gain data are exclusively low intensity halo returns surrounding edges of needles and branches (Figure 5).

At a distance of ~45 m, the high gain receiver begins to record returns that are clearly fine fuels and branchwood (as opposed to halo), and because of the scaling issues of the instrument, it becomes less feasible to separate foliage from branchwood for analysis. Due to the scaling issues of the intensity data for the ILRIS instrument as discussed previously, all results presented hereafter are based exclusively on low gain data.

3.2. Range Correction for Intensity

Backscatter intensity from a 98.7% albedo Spectralon® tile across an 85 m range from 15 to 100 m shows intensity decaying with range as an exponential function with an exponent of 0.038 (b: p = 0.0001 on 15 degrees of freedom; SE = 1.6%; Figure 6). Canopy fine fuel intensities follow a similar decay ($e^{-0.041}$; b: p = 0.0016 on 3 degrees of freedom; SE = 4.1%; Figure 6). The low gain distance normalization equation subsequently used in this study is:

$$\left(\frac{e^{(0.04*\left(\sqrt{x^2+y^2+z^2}\right))}}{e^{(0.04*dref^2)}} \right) * i_{raw} = i_{rc} \quad (1)$$

where *dref* is the reference distance equal to 15 m, i_{raw} is the raw intensity value, and i_{rc} is the range-corrected intensity. These findings differ somewhat from inverse-square law behavior reported elsewhere for the ILRIS [6], although Pfeifer *et al.* [16] have also shown that ILRIS intensity data do not follow $1/d^2$ at close ranges. Inside 40 m range, both the Spectralon and Douglas-fir data could be range-corrected reasonably using linear functions (Figure 6), confirming some of the generic findings of Kaasalainen *et al.* [8]. Figure 7 depicts the effects of the range correction for Spectralon and Douglas-fir samples. At 45 m, the Douglas-fir intensity distribution is compressed compared with other ranges because as the distance from the scanner increases, the low gain receiver registers

relatively fewer returns (Figure 7). The large positive outliers in the Douglas-fir samples depicted in Figure 7(c,d) are from branchwood, erroneously in the case of the fine fuels samples.

Figure 6. Relative intensity *vs.* target distance for a 98.7% albedo Spectralon tile, Douglas-fir fine fuel samples, and Douglas-fir intact branches. A hypothetical $1/d^2$ curve is shown for reference. An exponential curve best fits the Spectralon (r^2 = 0.988; SE 1.3–4.5%), canopy fine fuel (r^2 = 0.995; SE 1.9–5.1%), and intact branch data (r^2 = 0.997; SE 4.8–7.3%). The variability in standard errors is a function of range-dependent differences in sample sizes.

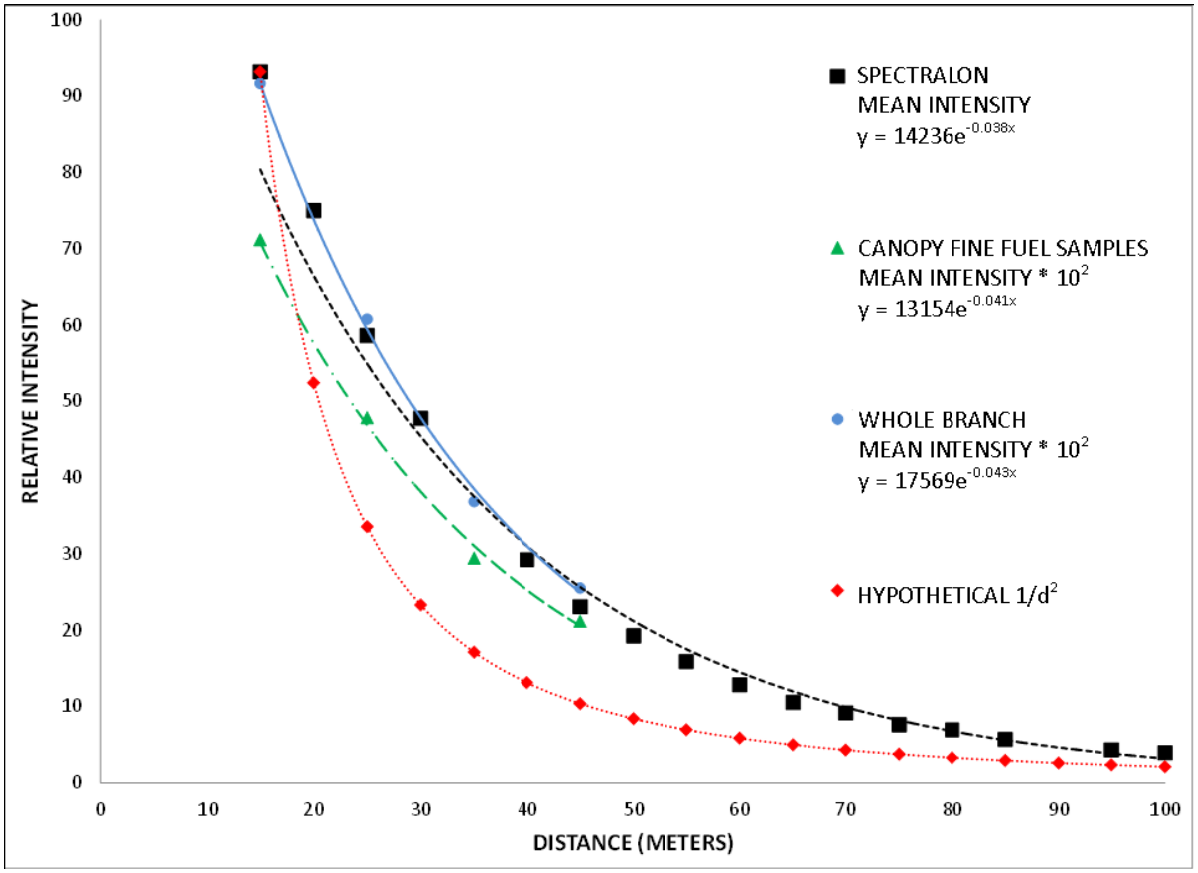

3.3. Range and Angle Effects on Intensity

Branch orientation affects whole-branch intensity, probably because of differences in visibility of fine fuels *vs.* branchwood due to shadowing (Figure 8(a)). The uniformity of intensity from larger branches was not evaluated directly, but angular effects are evident in scans of tree boles. Intensity displays more uniformity across branch orientations and ranges for fine fuels than for branchwood (Figure 8(b)), suggesting Lambertian reflectance properties for smaller particles.

It was not possible to test statistical equivalence between branches, angles, and ranges using non-parametric rank tests due to the occurrence of extreme outliers in some distributions. Further, the data normalization needed for traditional Analysis of Variance was ineffective. Therefore, the box-whisker plots depicted in Figure 8 stand alone as analysis, with the caveat that the samples can be rendered statistically equivalent in a Kendall Tau test by removing extreme outliers.

Figure 7. Box-and-whisker plots of intensity *vs.* target distance for a 98.7% albedo Spectralon tile and Douglas-fir whole branches and fine foliage in the 0° position. For each plot, the dark horizontal line represents the median value, and the grey box represents data from 25% to 75%. The fences extend to 1.5 times the height of each box and represent approximately 95% of the data. The circles are outliers, *i.e.*, data points that fall outside of the fence. Asterisks are extreme outliers, which are cases with values greater than three times the height of the box. **(a)** Raw Spectralon tile intensity *vs.* distance. **(b)** Range-corrected Spectralon tile intensity *vs.* distance. **(c)** Raw Douglas-fir fine foliage intensity *vs.* distance. **(d)** Range-corrected Douglas-fir fine foliage intensity *vs.* distance. **(e)** Raw Douglas-fir whole branch intensity *vs.* distance. **(f)** Range-corrected Douglas-fir whole branch intensity *vs.* distance.

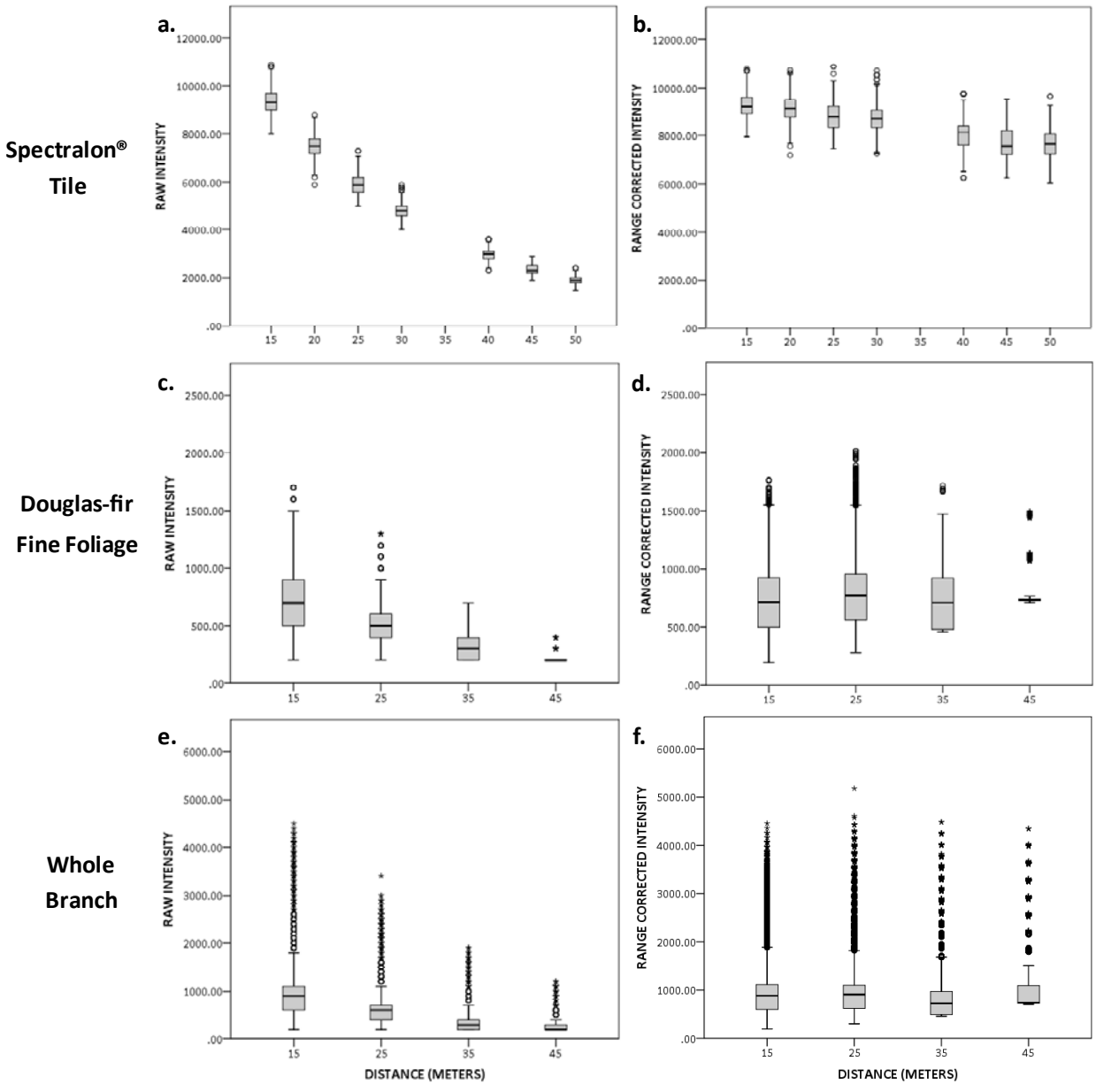

Figure 8. Box-and-whisker plots for whole-branch and canopy fine fuel intensities for lumped branch samples at 25 m across multiple angles. **(a)** Whole branch intensity *vs.* branch angle. Observed variations are likely due to differences in biomass shadowing based on the scan angle combined with instrument sensitivity. **(b)** Canopy fine fuel intensity *vs.* branch angle. Fine fuels show no systematic angular effects.

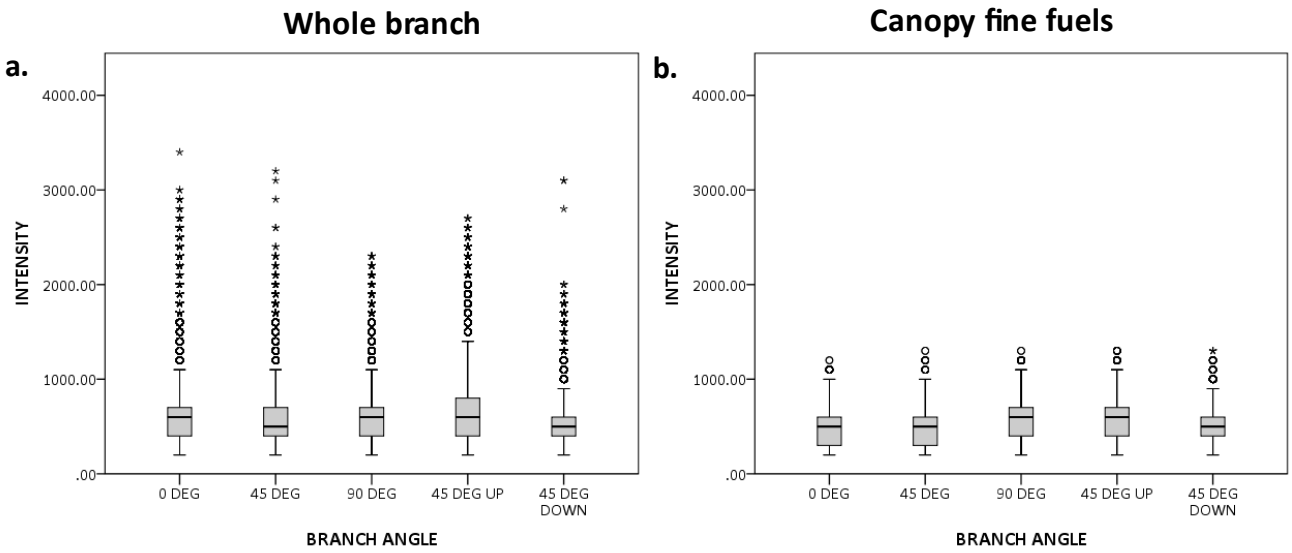

3.4. Discriminating Fine Fuels from Branchwood

Branchwood is characteristically brighter than fine fuels (Figure 9), suggesting that the size and shape of targets relative to the size of the laser footprint is a primary driver of intensity [6,7]. This result is counterintuitive in the context of optical remote sensing logic, in which foliage is characteristically highly reflective at near-infrared wavelengths due to leaf cell structure, but it is consistent with other data from airborne laser scanning [13]. It is also plausible that water content of foliage contributes to observed differences in intensity, as the laser wavelength is in a strong water absorption band. Additionally, fine fuels and branchwood have distinctly different intensity distributions, albeit with some overlap between classes. They can be distinguished from one-another using an intensity threshold equal to mean intensity plus one standard deviation (Figure 10) and with similar thresholds derived from both natural breaks and unsupervised classifications of intensity data (Figure 11). In short, TLS of Douglas-fir branches within ranges of 15–45 m produces low intensity reflections associated with small diameter material and high intensity reflections associated with larger diameter material. The difference in intensity between classes is large and distinctive, and the ability to produce comparable thresholds using a variety of different methods lends credibility to selection of a breakpoint between 1,000 and 1,100 DNs. Based on visual inspection of high resolution imagery coincident with laser scans, the positive outliers observed in the canopy fine fuels class (Figure 11) appear to be the result of including branchwood returns when fine fuel samples were selected from the laser point cloud, whereas the negative outliers in the branchwood class are returns on the edges of branches in which the laser footprint is fractionally occupied. Overall, branchwood is more likely to be misclassified as fine fuel than *vice versa*. Collectively, these results point to integration of TLS

geometric and intensity data with RGB-NIR data rendered on the point cloud from a calibrated camera mounted on the TLS as a potentially fruitful area of future research.

Figure 9. Box-and-whisker plot of grouped samples by size class at 25 m and 0°.

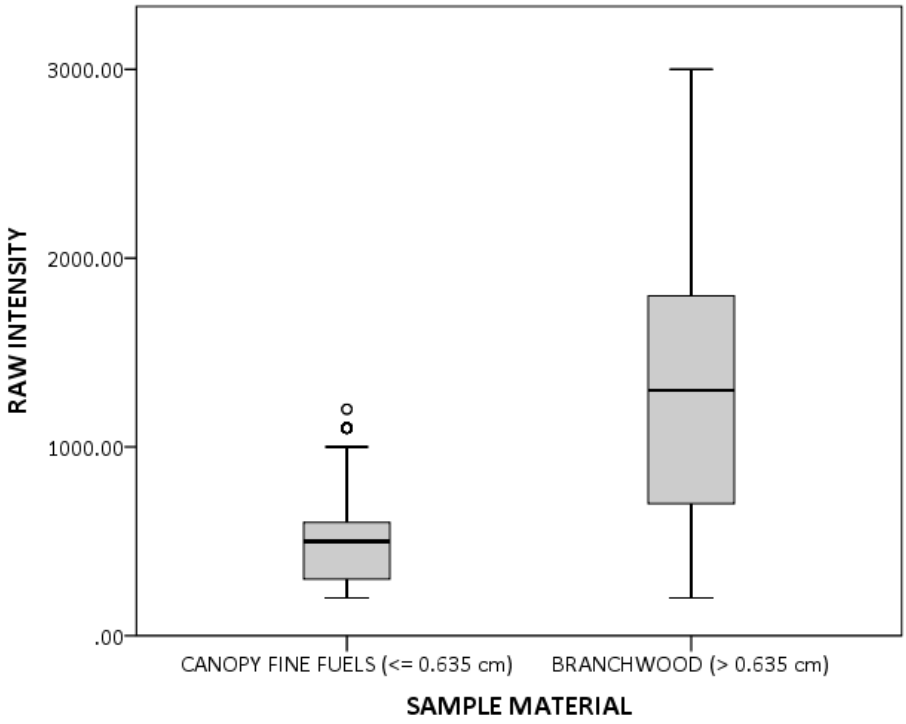

Figure 10. Histogram for all whole-branch Douglas-fir scans at 25 m and 0°, illustrating the canopy fine fuel intensity threshold equal to mean plus one standard deviation (red line).

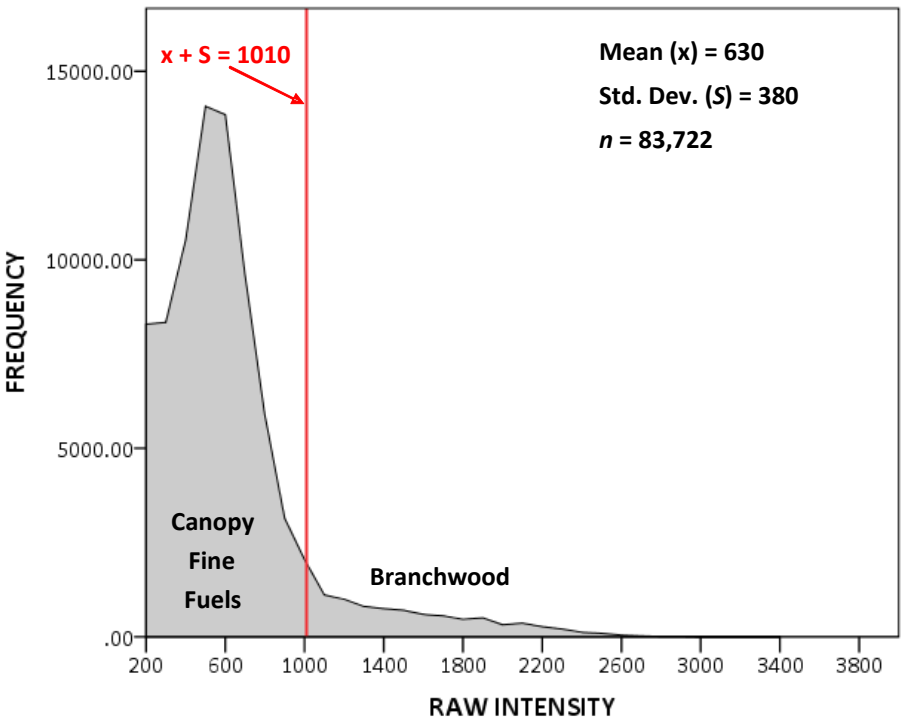

Figure 11. Classification of a Douglas-fir branch into intensity-based size class categories using different methods. For (a), (b), and (c), canopy fine fuel returns are shown in green and branchwood returns are shown in black. **(a)** High-resolution photograph of branch sample #3 in the 0° position. **(b)** Classified image edited to branch extent. Data are classified according to a threshold of 1,010, which is equal to one standard deviation above the mean for all branches scanned at 25 m and 0°. **(c)** Applying the Natural Breaks method with two classes in ArcMap produces a threshold equal to 1,000. **(d)** Unsupervised classification (ERDAS ISODATA, iteration threshold of 10) results in a similar threshold.

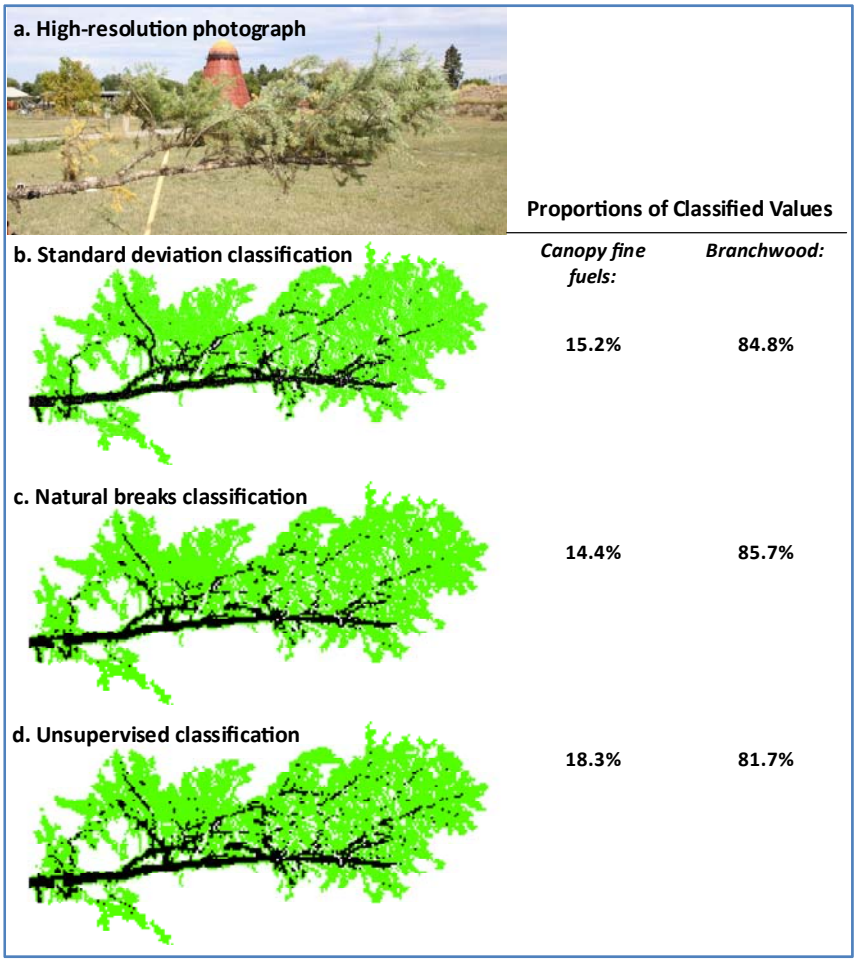

3.5. Biomass Models

The relationship between biomass of defoliated branches and TLS return density is linear (Figure 12). When fine fuels are included on the branch, model efficacy for branchwood declines somewhat as shadowing of branch features occurs (Figure 13), but the model remains linear and produces a larger standard error (~29% *vs.* ~21% of mean). Fine fuels (based on classified intensity) and total branch mass are similarly related to return density (Figure 13). Fine fuel model standard error is similar to the branchwood error produced by the defoliated branch (~23% *vs.* ~21%), and the total branch mass model error is somewhat larger (~25%) The performance of each model is predicated on the assumption that mass is predictably related to surface area, and observed variability in performance is likely caused by shadowing produced by 3-dimensional branch structure, variations in material

densities, and inconsistencies in the intensity-based classification of fuels by size class. These considerations notwithstanding, foliage, branch, and total biomass are predictable from intensity-classified return density at branch-scale.

Figure 12. Return density per branch *vs.* dry weight in grams for the defoliated branch scans at 25 m and 0° (r^2 = 0.986; SE 20.8%).

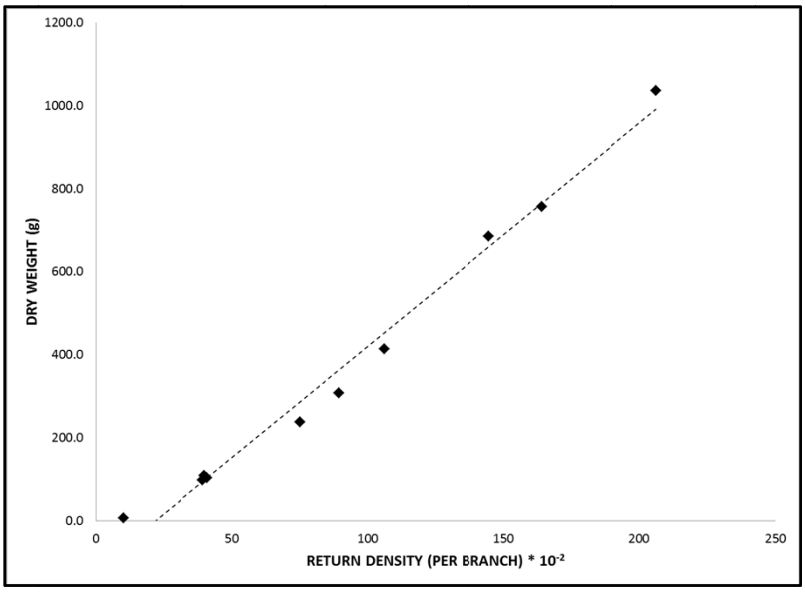

Figure 13. Return density per branch *vs.* dry weight in grams for fine fuels (intensity ≤ 1,010; r^2 = 0.898; SE 22.7%), branchwood (intensity > 1,010; r^2 = 0.937; SE 28.9%), and total returns (r^2 = 0.940; SE 25.5%) for intact branch scans at 25 m and 0°.

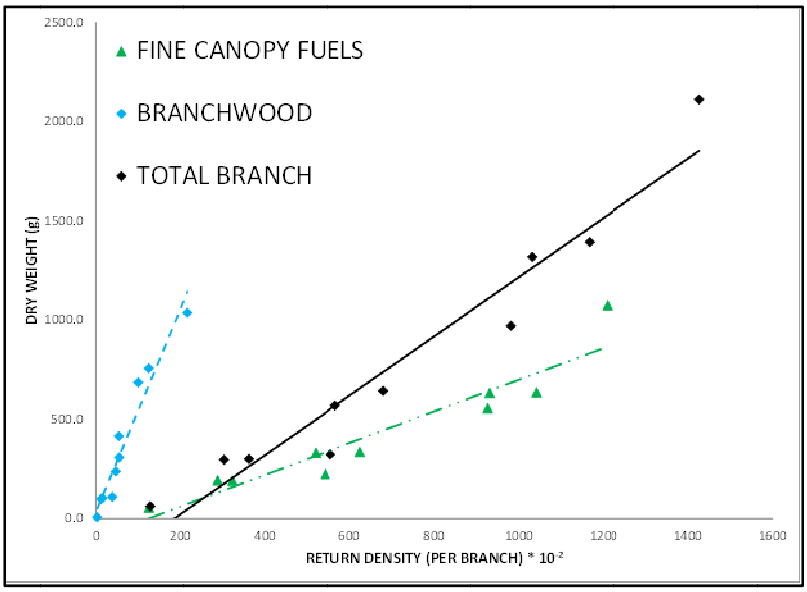

An examination of return density across branch orientations shows that branch angle impacts biomass prediction (Figure 14(a)). The relative slopes of each equation are logical, *i.e.*, angles that promote more shadowing (0°, 45°, 90°) result in larger slopes because the instrument registers fewer returns relative to total branch mass. Not surprisingly, for Douglas-fir the best orientation is 45° down,

which is a viewing geometry that exposes the entire branch structure. The 45° up orientation should produce equally good results, but this position was difficult to maintain on the tripod mounting structure, resulting in some questionable scans. We are cautious about interpreting these results without repetition utilizing a more robust mounting structure. Collectively, the results suggest that for individual branches, an angular correction for biomass would improve model performance. However, even if angle is not dealt with explicitly, return density still tracks biomass with sensible error (Figure 14(b)).

Figure 14. Angular effects on Douglas-fir branch biomass models. **(a)** Relative return density per branch *vs.* dry weight in grams for each of five branch sample angles: 0° (r^2 = 0.923; SE 26.7%), 45° (r^2 = 0.788; SE 92.2%), 90° (r^2 = 0.983; SE 42.6%), 45° up (r^2 = 0.262; SE 14.1%), and 45° down (r^2 = 1.00; SE 55.7%). **(b)** Relative return density per branch *vs.* dry weight in grams for all angled scans (r^2 = 0.721; SE 11.9%). Removing the problematic 45° up scans changes the regression and SE slightly (r^2 = 0.834; SE 14.6%).

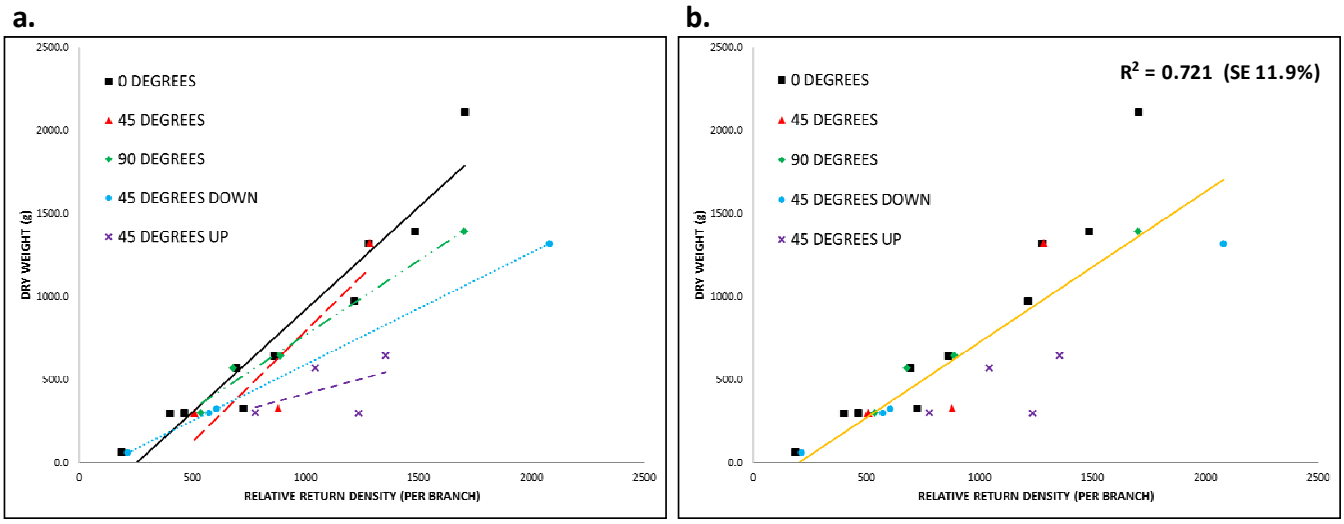

4. Conclusions

The use of TLS for discriminating crown fuels by size class using intensity data is apparent at branch-scale for Douglas-fir. Reflectance intensity appears to depend on the size and arrangement of particles relative to the size of the laser footprint, as noted in [7], while angle of incidence is a factor for objects with specular reflectance characteristics, such as smooth tree branches and boles. With respect to Douglas-fir, these behaviors can be exploited to distinguish foliage and small branches from larger branches and boles within ranges of 15 to 45 m using an Optech ILRIS scanner. Given the apparent importance of laser spot size in determining intensity [7], combined with the decay of reflected energy with distance, it is unlikely that our results will apply directly at longer ranges. For the instrument used in this study, laser spot size increases from 1.46 cm to 1.97 cm between 15 m and 45 m. For comparison, spot sizes at ranges of 100 m, 500 m, and 1,000 m are 2.90 cm, 9.70 cm, and 18.20 cm, respectively. Anecdotal results from long-range scans of coniferous forest depict trees close to the scanner with needles and small branches fully enumerated, while the trees near the edge of

illumination extinction (~700 m) exhibit only large branches and boles (e.g., foliage and small branches become increasingly transparent to the laser with range).

By using an intensity threshold to classify fine fuels and branchwood, it also appears possible to predict fuel mass by size class from laser density data. The linear models relating fuel mass to density produced errors of ~25% of the mean for both size classes of fuels and for total branch. While scan angle affects model performance primarily due to shadowing of background elements by material in the foreground, ignoring it still produces a high coefficient of determination and a standard error of about 14% of mean mass. Given the systematic orientation of branches around tree boles, it may be possible to correct for angle on scans of whole trees. It is worth noting that the improvement in standard error in the model that includes scans at all angles reflects a relatively large sample size and draws attention to limitations of our study with respect to small samples. Ten branches from ten trees within a single stand and four scans per angle class are inadequate to enumerate fully density-mass relations for Douglas-fir, but they provide a starting point for using TLS to characterize biomass/fuels by size class for trees.

Although we are confident in the ability to distinguish fine fuels from branchwood for whole trees using the techniques developed in this paper, it is not yet evident whether biomass will be predictable at tree-scale. Scaling functions from branch to tree have not yet been investigated, and it is not clear whether the shadowing that occurs within laser scans of tree crowns will bias predictions of biomass amount and/or location. This is an area of ongoing research. In a related area, differences between tree species have not been characterized, but various conifer specimens appear dissimilar in laser scans (Figure 15). Consequently, we anticipate distinctive intensity-density-mass relations for each species.

Additionally, we acknowledge that the density-mass relationships documented in this paper are attributable to that fact that branch surface area and mass are related. This is to say, mass is a modeled derivative of return density that is conventional and relatively easy to measure in the field, but surface area is the more direct measurement from TLS. Given that many fire behavior models require surface area inputs in addition to mass and volume, TLS may ultimately prove advantageous for characterizing fuelbeds, with the caveat that validation of such measurements will be difficult.

Lastly, using TLS to characterize forest properties inevitably requires a detailed understanding of scanners that were not designed for this purpose. Thus, one motivation for our study was to improve understanding of the Optech ILRIS instrument for a growing forestry user community. However, because there are several different scanners used by the research community that operate in visible and near-infrared wavelengths and a general reluctance by manufacturers to share information with users, there is a constant struggle to understand which results are scanner-specific and which are portable. While some of the results in our study apply specifically to the ILRIS, the primary utility in our findings comes from the demonstration that conifer tree materials of different sizes and arrangements produce characteristic reflectance intensities that most likely result from the interaction between target size/shape and laser spot size. By demonstrating with a single species and a single TLS system we have shown that there is analytical value in intensity data associated with scans of conifer branches, related to distinguishing biomass by size class, as well as for predicting biomass by size class from return density. We propose that this approach should be portable to other scanners and may lead to fast, highly automated procedures of tree/forest survey, data analysis, and classification.

Figure 15. Laser scans of 2 m tall conifer specimens of different species at 25 m. **(a)** Douglas-fir (*Pseudotsuga menziesii*), **(b)** lodgepole pine (*Pinus contorta*), and **(c)** ponderosa pine (*Pinus ponderosa*).

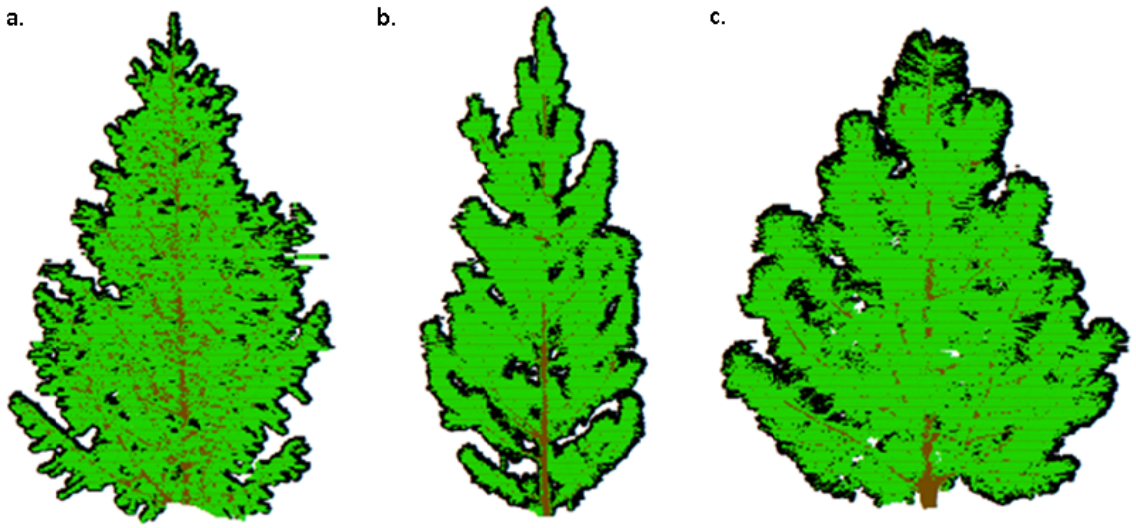

Acknowledgements

The authors of this paper wish to acknowledge the National Center for Landscape Fire Analysis, the Wildland Fire Science Partnership, and the Joint Fire Sciences Program (Project 10-1-02-13) for support of this work.

References and Notes

1. Hopkinson, C.; Chasmer, L.; Young-Pow; C.; Treitz, P. Assessing forest metrics with a ground-based scanning lidar. *Can. J. Forest Res.* **2004**, *34*, 573-583.
2. Watt, P.; Donoghue, D. Measuring forest structure with terrestrial laser scanning. *Int. J. Remote Sens.* **2005**, *26*, 1437-1446.
3. Danson, F.; Hetherington, D.; Morsdorf, F.; Koetz, B.; Allgower, B. Forest canopy gap fraction from terrestrial laser scanning. *IEEE Geosci. Remote Sens. Lett.* **2007**, *4*, 157-160.
4. Affleck, D.; Seielstad, C.; Sanchez-Meador, A.; Goodburn, J.; Queen, L.; Keane, R. *Characterizing Crown Biomass and Crown Density Profiles in Conifer Forests of The Interior Northwest*; Project 10-1-02-13; Joint Fire Science Program: Boise, ID, USA, 2010.
5. Gregoire, T.; Valentine, H. *Sampling Methods for Natural Resources and the Environment*; Chapman & Hall/CRC: Boca Raton, FL, USA, 2008.
6. Franceschi, M.; Teza, G.; Preto, N.; Pesci, A.; Galgaro, A.; Girardi, S. Discrimination between marls and limestones using intensity data from terrestrial laser scanner. *ISPRS J. Photogramm.* **2009**, *64*, 522-528.
7. Pesci, A.; Teza, G. Effects of surface irregularities on intensity data from laser scanning: An experimental approach. *Ann. Geophys.: Italy* **2008**, *51*, 839-848.
8. Kaasalainen, S.; Krooks, A.; Kukko, A.; Kaartinen, H. Radiometric calibration of terrestrial laser scanners with external reference targets. *Remote Sens.* **2009**, *1*, 144-158.

9. National Wildfire Coordinating Group. *Glossary of Wildland Fire Terminology*; National Interagency Fire Center: Marana, AZ, USA, 1996; p. 162.
10. Keane, R.; Reinhardt, E.; Scott, J.; Gray, K.; Reardon, J. Estimating forest canopy bulk density using six indirect methods. *Can. J. Forest Res.* **2005**, *35*, 724-739.
11. Hosoi, F.; Omasa, K. Voxel-based 3-D modeling of individual trees for estimating leaf area density using high-resolution portable scanning lidar. *IEEE Trans. Geosci. Remote Sens.* **2006**, *44*, 3610-3618.
12. Loudermilk, E.L.; Hiers, J.; O'Brien, J.; Mitchell, R.; Singhania, A.; Fernandez, J.; Cropper, W., Jr.; Slatton, K. Ground-based LIDAR: A novel approach to quantify fine-scale fuelbed characteristics. *Int. J. Wildland Fire* **2009**, *18*, 676-685.
13. Suratno, A.; Seielstad, C.; Queen, L. Tree species identification in mixed coniferous forest using airborne laser scanning. *ISPRS J. Photogramm.* **2009**, *64*, 683-693.
14. The Python Standard Library. 9.6. random—Generate pseudo-random numbers. Available online: http://docs.python.org/release/2.6.6/library/random.html (accessed on 9 May 2011).
15. Hosoi, F.; Omasa, K. Factors contributing to accuracy in the estimation woody leaf area density profiles using portable lidar imaging. *J. Exp. Bot.* **2007**, *58*, 3464-3473.
16. Pfeifer, N.; Höfle, B.; Briese, C.; Rutzinger, M.; Haring, A. Analysis of the backscattered energy in terrestrial laser scanning data. In *The International Archives of the Photogrammetry, Remote Sensing and Spatial Information Sciences*; ISPRS: Vienna, Austria, 2008; Volume XXXVII, pp. 1037-1044.